Wearable Physical Sensors for Non-invasive Health Monitoring

Cong Thanh Nguyen, Khoa Tuan Nguyen, Toan Dinh, Van Thanh Dau, and Dzung Viet Dao

1 Introduction

Advances in sensing technology have revolutionized the way we approach health care, with a particular focus on non-invasive methods for monitoring and managing our health. Among the remarkable breakthroughs in this field, wearable sensors have emerged as a promising solution, enabling continuous and real-time health monitoring. These sensors use various sensing mechanisms to gather physiological data and provide valuable insights into our well-being.

This chapter presents wearable physical sensors for non-invasive health monitoring, exploring the sensing mechanisms used, the concepts and capabilities of human motion monitoring sensors, the advancements in heart rate and blood pressure sensors, and the respiratory sensors. By understanding the principles behind these sensors and their applications, we can unlock new possibilities for personalized health care, early disease detection, and improved well-being.

The chapter is structured into four sections, each focusing on its key aspects as follows.

Section 2 introduces a wide range of sensing mechanisms or sensing effects which are used in wearable sensors for non-invasive health monitoring.

Section 3 explores the structure and working principle of sensors used for human motion monitoring, with a specific focus on Micro Electromechanical Systems (MEMS) sensors. One of fundamental aspects of health monitoring is understanding human motion and activity. Human motion monitoring sensors, such as accelerometers, gyroscopes, and magnetometers, enable the assessment of physical activity levels, gait analysis, and the detection of abnormal movements. These sensors

C. T. Nguyen · K. T. Nguyen · T. Dinh · V. T. Dau · D. V. Dao (✉)
School of Engineering and Built Environment, Griffith University, Parklands Drive, Southport, QLD 4222, Australia
e-mail: d.dao@griffith.edu.au

K. Mitsubayashi (ed.), *Wearable Biosensing in Medicine and Healthcare*,
https://doi.org/10.1007/978-981-99-8122-9_6

integrated into wearable devices can accurately track and analyze an individual's movements throughout the day.

Section 4 introduces heart rate and blood pressure sensors. The cardiovascular system plays a vital role in our overall health, making heart rate and blood pressure crucial parameters to monitor. Wearable sensors equipped with heart rate and blood pressure monitoring capabilities offer a non-invasive means of tracking these vital signs in real time. This section examines the different sensor technologies used for heart rate and blood pressure monitoring and explores their potential applications in non-invasive health monitoring.

Section 5 discusses the advancements in respiratory sensing technologies and their applications in wearable devices for non-invasive health monitoring. Respiratory function is a key indicator of overall health and plays a pivotal role in diagnosing and managing various conditions. Wearable respiratory sensors have the potential to monitor respiratory patterns and detect abnormalities without the need for invasive procedures. These sensors, such as strain gauges, chest bands, and respiratory sensors, offer a non-invasive approach to respiratory monitoring.

2 Physical Sensing Mechanisms for Health Monitoring

Different functional activities of the human body can be considered as stimuli for transducing into electrical signals, such as heart rate, blood pressure, breath, joint movement, and so on. A large number of wearable sensors have been developed to monitor these stimuli based on different sensing mechanisms, including piezoresistive, thermoresistive, capacitive, piezoelectric, triboelectric, and optoelectronic effects. The working principles of these sensing effects are presented in this section.

2.1 Piezoresistive Effect

The electrical resistance of a resistor is computed as a function of the resistivity (ρ), length (l), width (w), and thickness (t) as below

$$R = \rho \frac{l}{wt} \tag{1}$$

The change in the resistivity and dimensions of the resistor causes the alteration in the electrical resistance as below

$$\frac{\Delta R}{R} = \frac{\Delta \rho}{\rho} + \frac{\Delta l}{l} - \frac{\Delta w}{w} - \frac{\Delta t}{t} = \frac{\Delta \rho}{\rho} + (1 + 2\gamma)\varepsilon \tag{2}$$

Table 1 Longitudinal gauge factor of typical metals and semiconductors

Materials	Longitudinal gauge factors	References
Aluminum	3.1	[1]
Copper	2.9	[1]
Gold	4.48	[1]
p-Si [110]	120	[2]
n-Si [100]	−133	[2]
p-Ge [111]	105	[2]
n-Ge [111]	−155	[2]
n-GaAs [111]	−8.9	[2]

where γ is Poisson's ratio of the material and $\varepsilon = \Delta l / l$ is the strain in the longitudinal direction.

Piezoresistive effect is the change in the electrical resistance under the applied mechanical stress or strain. Gauge factor (GF) is commonly used to quantify the piezoresistive effect, which is defined as below

$$GF = \frac{\Delta R/R}{\varepsilon} = \frac{\Delta \rho/\rho}{\varepsilon} + (1 + 2\gamma) \tag{3}$$

As the resistivity of metals changes slightly under the applied strain, the gauge factor of metals is quite small and mainly depends on the mechanical/geometric properties. In contrast, the charge carrier mobility of semiconductors changes significantly under the applied stress or strain, resulting in a significant change in the resistivity or conductivity. Table 1 shows the GF of typical metals and semiconductors.

The piezoresistive effect in semiconductors has been investigated since the first experiment on the effect of strain on the electrical conductance of germanium and silicon [3], followed by other theoretical studies. So far, the theoretical models of the charge carrier mobility change under the applied stress or strain have been used to explain the piezoresistive effect in semiconductors [4]. The general idea is that the stress-induced modification of energy band diagram of semiconductors causes the repopulation of charge carriers (holes or electrons) in the valence band and conduction band, leading to the change in charge carrier effective mass and mobility, consequently changing the conductivity [5].

2.2 Thermoresistive Effect

Thermoresistive effect is the change in electrical resistance with the temperature variation. Therefore, the resistance is calculated as a function of temperature as below

$$R = R_0\left(1 + \alpha \Delta T + \beta \Delta T^2 + \ldots\right) \tag{4}$$

where α is the linear thermoresistive coefficient and β is the quadratic thermoresistive coefficient.

The resistance of metals increases with temperature ($\alpha > 0$), which is so-called positive temperature coefficient of resistance (TCR). Low-doped semiconductors have negative TCR since a large number of generated electrons and holes at elevated temperature reduce the resistivity. Nevertheless, highly doped semiconductors could have a positive TCR while they behave like metals and show small positive TCR at very high doping (metallic degeneration).

Thermistors are created for extremely high TCR. Metal oxides, which are used to make negative TCR thermistors, have considerably greater TCR than metals but also highly nonlinear characteristics. These metal oxides are used to develop small resistive temperature sensors. Some ceramic materials have high positive TCR, so these materials change from low resistivity to high resistivity within a few degrees. These ceramic materials are employed as temperature switches to protect electronic circuits from overcurrent.

2.3 Capacitive Effect

The capacitance between two parallel conductive plates is calculated below

$$C = \frac{q}{V} = \epsilon \frac{A}{d} \tag{5}$$

where q, V, A, d are the charge, voltage, overlap area, and distance between the two plates, and ϵ is the permittivity of the material between the two plates, defined as

$$\epsilon = \epsilon_0 \kappa \tag{6}$$

where ϵ_0 is the electric constant and κ the dielectric constant.

The capacitive effect is the change in the capacitance between two conductive plates, caused by the change in the distance (Δd), overlapped width (Δw), overlapped length (Δl), and permittivity ($\Delta \epsilon$) between the plates. To maintain simplicity, both w and l are generally kept constant ($\Delta w = 0$, $\Delta l = 0$). Therefore, the capacitance is computed as below

$$C = (\epsilon + \Delta\epsilon) \frac{wl}{d - \Delta d} \tag{7}$$

where $\Delta\epsilon$ is the change in permittivity of the dielectric material and Δd represents the change in the distance between the parallel plates.

The capacitance relies not only on the physical deformation (Δd) but also the permittivity ($\Delta \epsilon$). Depending on the chosen dielectric material, the capacitance

between two plates can be greatly affected by temperature or humidity which alters the permittivity significantly [6–8].

2.4 Piezoelectric Effect

Piezoelectric effect is the creation of mechanical deformation in some non-conductive materials in reaction to the application of an electric field, or the creation of electric charges on the surface of such materials when they experience a mechanical stress.

The piezoelectric effect can also be interpreted as electromechanical interactions between mechanical states and electrical states. Here, piezoelectric constants are defined to represent these linear and proportional relations. With the piezoelectric constants being in the form of third-rank tensors, the electric field and displacement as first-rank tensors, and the stress and strain as second-rank tensors, the piezoelectric relations are formulated as below ($i, j, k = 1, 2, 3$)

$$D_k = d_{kij} T_{ij} \tag{8}$$

$$S_{ij} = d^*_{kij} E_k \tag{9}$$

where D_k and E_k are the electric displacement and electric field, S_{ij} and T_{ij} are the strain and stress components, and d_{kij} and d^*_{kij} are the piezoelectric charge and strain constants.

The indexes of piezoelectric constants are generally represented by the reduced Voigt notation d_{km} with the index k designated for the electric displacement or electric field component in a reference Cartesian coordinate system (x_1, x_2, x_3), and $m(1, \ldots, 6)$ for specifying the stress or strain. Specifically, $m = 1, 2, 3$ stand for the normal stresses along axes x_1, x_2, x_3, while $m = 4, 5, 6$ are for the shear stresses T_{23}, T_{13}, T_{12}, respectively. Both d_{km} and d^*_{km} are the piezoelectric constants, however their units are different.

2.5 Triboelectric Effect

Triboelectric effect is a type of contact electrification happening when certain materials are electrically charged after they contact and then separate from other materials. Depending on different characteristics, i.e., the selected material, surface roughness, exerted stress, the polarities, and strengths of the created electric charges are different. For instance, amber can acquire an electric charge by the process of contact and separation with other materials like wool. Glass and silk, or hard rubber and fur, are other examples of materials obtaining a significant charge when rubbed together.

Triboelectric materials are commonly listed according to the polarity of charge separation when in contact with another material [9]. In this list, a material near the bottom will acquire larger negative charge when it touches another one close to the top, and vice versa. In other words, the greater the charge is transferred, the further away two materials are from each other on the list. On the other hand, materials near each other on the list may not exchange any charge or may exchange the opposite of what is implied by the list. This depends more on other factors than the type of material, such as rubbing, contaminants, and other properties.

2.6 Optoelectronic Effects

2.6.1 Photoconductive effect

Photoconductive effect is the change in the conductivity or resistivity of semiconductors under the light illumination. This is explained by the generation of electron–hole pairs when incident photons are absorbed into the materials. Here, the photoconductivity is defined as below

$$\sigma = q(\mu_e n + \mu_h p) \tag{10}$$

where q is the electric charge, μ_e and μ_h are the mobilities of electrons and holes, $n = n_0 + \Delta n$ and $p = p_0 + \Delta p$, where n_0 and p_0 are the concentrations of electrons and holes in the dark condition, and Δn and Δp are the created electrons and holes under the light excitation.

The number of photogenerated charge carriers ($\Delta n = \Delta p$) can be expressed as

$$\Delta n = \eta \frac{\alpha \cdot I \cdot \tau}{h\nu} \tag{11}$$

where $\eta, h\nu, \alpha, I$, and τ are the quantum efficiency, incident photon energy, absorption coefficient, illumination intensity, and carrier lifetime, respectively.

2.6.2 Photovoltaic effect

Photovoltaic effect is the generation of output voltage across p–n junctions under the light illumination. The phenomenon is explained by the creation of electron–hole pairs in the p–n junctions when illuminated by certain wavelengths. The created electrons then move to the n-side while the generated holes transport oppositely toward the p-side of the p–n junctions. The accumulation of photogenerated holes and electrons in two sides of the p–n junction generates the output voltage [5, 10].

3 Human Motion Monitoring Sensors

3.1 Importance of Human Motion Monitoring

Human motion is a vital physical capacity which is crucial for a large number of daily activities. However, human mobility may be compromised by injury, aging, or illness progression. In healthcare applications, the accuracy of characterizing human motion is vital to diagnose, categorize, and manage a wide range of movements and physiological disorders. Recently, the change in human movement has been considered as a key factor not only in common and chronic diseases, such as heart failure, diabetes, and stroke, but also in some motion disorders, such as Parkinson's disease and Huntington's disease [11]. Therefore, maintaining and rehabilitating human motion have been considered as an essential part of disease management. An essential factor for enhancing motion rehabilitation in health care is to accurately characterize comprehensive human motion. Thus, the function of human motion monitoring sensors is to acquire real-time data, and then process to characterize related movements.

In the past, human motion monitoring mostly relied on image processing, which is known as camera-based human motion capture [12]. In this case, the movement of multiple sensing elements attached to the body is used to determine the body motion. This technique is effective; however, incorporating it into contemporary medical systems, such as portable medical devices, is expensive and obtrusive. Other widely used human mobility management sensors were wrist-worn systems which tracked simple activities and provide data on aspects of body translation, for instance the total step number and travel distance. Nevertheless, detailed analyses of the movements of local body parts, such as arms or legs as well as their velocity, acceleration, or rotational parameters, are necessary to properly characterize and comprehend biomechanics and other complicated movements. Alterations in movements of these components may be associated with disease, atrophy, and injury, while tracking the recovery progress is crucial for effective rehabilitation.

In recent years, substantial advancements in microscale motion sensing technology have greatly aided the development of human balance prostheses, sports medicine, radiotherapy, and biomechanical research [13–15]. Specifically, strong toolkits for body motion detection have been made possibly by the fast development of MEMS sensors with high precision, high reliability, and various functionalities. Over the past two decades, MEMS sensors for motion monitoring have drawn a lot of attention and are still a thriving research field.

3.2 Human Motion Monitoring Sensors and Methods

The most prevalent uses of human motion monitoring sensors are in the field of health care. These applications include gait monitoring and motion capture. The most

frequent use is for gait assessment because of its connection to cognitive impairments. Besides, motion capture is used to gather data on human kinematics for motion analysis or to look for potential illnesses.

3.2.1 Gait Monitoring

Gait analysis is currently a critical task in therapeutic and rehabilitation programs because it supplies extensive knowledge about the gait quality, the behavior of the gait pattern, and other dynamic aspects. The results of a gait study might also provide information on a specific gait disease or impairment. Based on that analysis, customized therapies can be suggested. Currently, the most common wearable sensors developed for monitoring human motion consist of inertial sensors, ultrasonic sensors, and laser rangefinder systems.

Inertial sensors are becoming prevalent in studies of human mobility. An inertial measurement unit (IMU) combining accelerometers, gyroscopes, and magnetometers is the most common inertial sensors. Attaching to body parts such as chest, arms, or legs, an IMU is capable of measuring their acceleration, rotation, and gravitational force. Estimates of the gait phases and spatiotemporal characteristics can be made using these parameters. IMUs are extremely resilient sensors since they integrate multiple sources of data, yet they frequently need sophisticated fusion algorithms to produce better estimations.

Accelerometers are the most popular choice when an outpatient gait analysis is needed. They have significant benefits including compact size, high mobility, low cost, and low energy consumption. Accelerometers can be used for both translation and rotational motions either with uniaxial or multi-axial configurations. These sensors work based on Newton's second law of motion and Hooke's law. Different sensing effects have been applied to develop accelerometers, such as piezoresistive effect, capacitive effect, and piezoelectric effect. For example, a piezoresistive accelerometer consists of a proof mass hung on surrounding beams which are fixed at the middle to the frame, Fig. 1(a) [16, 17]. Nanowire p-type silicon piezoresistors are embedded on the sensing beams. In human gait analyses, this piezoresistive accelerometer is attached to a specific position of a human part. Depending on the human motion, the gravitational force deforms the surrounding beams of the accelerometer differently. This results in the resistance change of the piezoresistors, which is converted to the change in output voltage by using the Wheatstone bridge circuit.

Gyroscopes are sensors for measuring the angular velocity, using the Coriolis effect to convert the rotational velocity to a measurable linear motion. This velocity is not affected by the gravitational force. The structure of a symmetric and decoupled gyroscope consisting of a proof mass hung by two sets of springs placed in perpendicular directions is presented in Fig. 1(b) [18]. This creates two mass-spring systems in perpendicular directions, working as linear accelerometers. However, these systems have different functions of driving mode and sensing mode. Upon the rotational movement of the frame around the third axis, the created Coriolis acceleration in

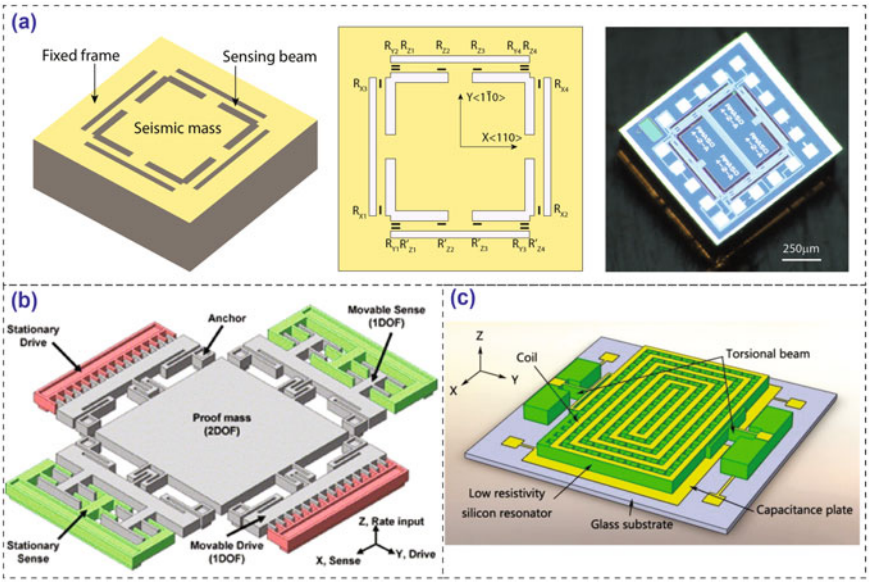

Fig. 1 **a** A three degrees of freedom MEMS piezoresistive accelerometer, **b** Design of a vibratory gyroscope; and **c** Design of a Lorentz-force MEMS magnetometer. Reproduced with permission from [17–19]

the orthogonal orientation of the driving mode provides the input which is measured by the sensing mode accelerometer. In gait analysis applications, gyroscopes can be applied to measure the periodic and repeated rotational movement of different body parts. Current commercial inertial sensors with accelerometer and gyroscope can measure six degrees of freedom of both linear accelerations and rotational speeds.

Magnetometers, which measure changes in magnetic fields, are typically the third sensing component of an IMU. These instruments measure the air magnetic flux density and identify variations in the Earth's magnetic field. For example, the design of a torsional resonant magnetometer is illustrated in Fig. 1(c), working based on the Lorentz-force principle [19]. This magnetometer is fabricated on a glass substrate, consisting of a coil, torsional beams, capacitance plates, and silicon resistors. When the electrical current in the coil is placed in an external magnetic field, the generated Lorentz force causes the displacement of the torsional structure. This displacement is measured by two sensing capacitors fabricated on the torsional structure, then the external magnetic field can be determined. Magnetometers are often employed to improve the accuracy of IMUs by determining the direction toward Earth's magnetic North. Commercial inertial sensors with accelerometer, gyroscope, and magnetometer are considered as nine degrees of freedom IMUs.

Ultrasonic range sensors determine the distance to a target object by converting the reflected sound of ultrasonic waves to a measurable electrical signal. For example, gait parameters are estimated by determining the distance between human feet and

the ground [20]. Other parameters that can be measured consist of the step length, stride length, and distance between two steps.

Laser range finders are optical sensors that measure the distance of an object using infrared laser beams. These systems typically comprise a transmitter that sends out laser pulses on a rotational frame to measure distance at various angles. The required duration since the laser beam is sent out reaches the object, then goes back, and is recorded according to the time-of-flight principle. For example, these sensors are positioned in the user's front at about his knee level to track the position of user legs in walker-assisted applications [21].

3.2.2 Joint Movement Monitoring

Among different wearable techniques in joint movement analysis, there are three most prevalent used sensors, including optical sensors, inertial sensors, and textile-based sensors.

Optical sensors measure the alteration in light transmittance. Optical sensors consist of three main parts: a light source, an optical fiber, and a photodetector, Fig. 2(b) [22]. A light beam is generated by the light source, then its intensity after traveling through the optical fiber is measured by the photodetector. To monitor the joint movement, the light source and photodetector are attached on the upper half and lower half of a joint. By measuring the attenuation of beam intensity, the optical sensor can determine how the optical fiber is bent. The immunity to electromagnetic noises is a significant advantage of optical sensors in comparison with other methods.

Inertial sensors including accelerometers, gyroscopes, and magnetometers are normally integrated in an IMU. In this case, the joint alignment using two IMUs must be applied to calculate a joint angle accurately, Fig. 2(a) [22]. First, typical joint movements are based on to define a collection of postures for aligning these IMUs. The calculation of the joint angle is then obtained by fusion algorithms. Later, based on the data achieved by these algorithms, errors are assessed by comparing with those of a reference system. Finally, calibration functions are proposed to compensate

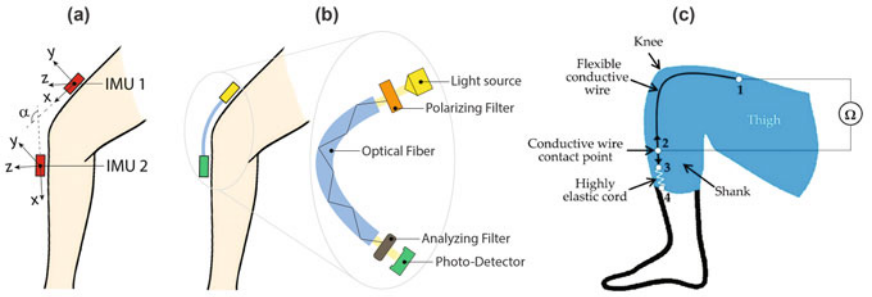

Fig. 2 Placement of **a** inertial sensors, **b** optical fiber sensors, and **c** flexible conductive wire for joint movement monitoring. Reproduced with permission from [22, 23]

the errors. This technique can be used to track complicated movements of different joints, such as elbow, ankle, and knee.

Textile-based sensors for example flexible conductive wire and strain sensors are ideal for making wearable joint monitoring systems. These sensors work based on the monitor of resistance change which corresponds to the joint angle. Textile-based sensors are a great option to create wearable monitoring devices because of their flexibility, simple structure, and easy integration into stretchable skin-tight fabrics. For instance, a flexible conductive wire sensor was integrated into stretchable garments for joint bending measurement, Fig. 2(c) [23]. In this case, a single conductive wire was fabricated in the fabrics around the knee, then the resistance change of this wire was measured to determine the knee bending. Another example is a textile-based wearable strain sensor that employed conductive yarns as a sensing element. A variety of textile-based materials with preferred conformability and elasticity were selected for developing wearable systems.

4 Wearable Heart Pulse and Blood Pressure Sensors

4.1 Importance of Heart Rate and Blood Pressure Monitoring

As the central organ of the circulatory system, the heart pumps blood that carries oxygen and nutrients to all parts of the body. Therefore, measuring heart rate and blood pressure can provide valuable data to predict potential cardiovascular diseases such as atrial fibrillation, coronary heart disease, heart attack, heart failure, and stroke. With rapid technological developments in materials, devices, and integration, wearable heart rate sensors have been becoming mainstream devices for continuous and real-time monitoring of heart conditions. Currently, heart rate monitoring is a must-have function in commercial wearable devices, such as Apple Watch, Fitbit, and smart bands [24, 25]. Most of these commercial devices utilize either optical-based—photoplethysmography (PPG)), or electrical-based—electrocardiography (ECG) transducers. The former technology monitors the heart rate by the reflection of light beams penetrating the blood flow through arteries, whereas the latter measures the body electrical signals to estimate the heart rate. Despite the tremendous commercialization progress of these two technologies, there are considerable obstacles that hinder their accuracy and reliability. For instance, due to employing optical-based methods, PPG is greatly affected by ambient lights, skin tones/colors, relative distance between devices, and the artery; meanwhile, ECG strictly requires multiple electrodes attached to the skin that typically cause discomforts and reduced performance with wearing durations due to sweat and the varying skin contact. To break through the current limits, tremendous efforts in device development and integration have been devoted toward high precision, and miniaturization wearable heart rate monitoring devices. For instance, strain-based MEMS heart rate sensors [26,

27] were introduced that can accurately measure blood pressure and pulse waves without the skin effect. Beyond the widely available information regarding commercially available PPG- and ECG-based devices, this section will focus on the latest research on micro-electromechanical system (MEMS)-based wearable sensors for heart pulse monitoring (HPM) or blood pressure monitoring (BPM).

4.2 Heart Rate and Blood Pressure Sensing Methods

Monitoring blood pressure and heart pulse can provide a range of quantitative evaluations and diagnostics for cardiovascular diseases and health conditions. Compared with inflatable brachial arm cuffs, wearable sensors yield real-time, continuous data for the variation of blood pressure during daily activities or exercise so that more insightful quantification of heart conditions can be gathered [30]. Blood flow is cycled around the body by a periodic pump pressure from the heart. A BPM sensor typically acts as a strain transducer unit placed on a skin site just above a blood artery, Fig. 3(a). When the heart pumps a blood flow, blood vessels expand and lead to the deformation of skin and the sensor. The sensor then translates the mechanical deformation into electrical signals (i.e., resistance, capacitance, voltage, triboelectric, and optical) recorded by electronic circuit and data logging units. This artery pulse waveform can be extracted as non-invasive medical diagnosis information containing the heart rate, arterial blood pressure, and blood vessel stiffness [31, 32]. These data are useful for the prediction of cardiovascular diseases such as atherosclerosis, coronary heart disease, and peripheral arterial disease [29].

There are two stages of a pulse waveform: the ascending and descending stages. The ascending stage corresponds to the expansion of the artery during the ventricular contraction, whereas the descending stage occurs with ventricular diastole, Fig. 3(b). Corresponding to different states, the blood pressure varies as a waveform with three distinct "waves": percussion (P) wave, tidal (T) wave, and diastolic (D) wave, Fig. 3(c). As such, P-wave and T-wave are the early and late stages of the systolic

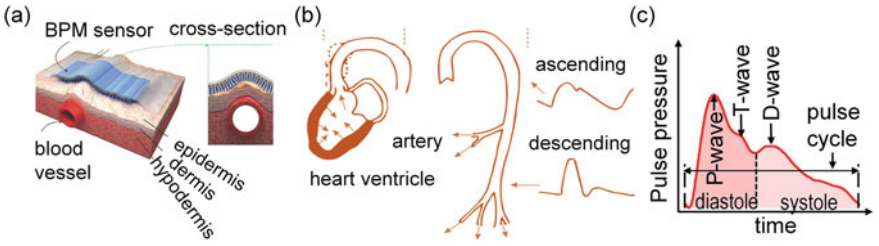

Fig. 3 **a** Working principle of blood pressure sensing: planar sensor placed just above a blood artery to sense its deformation upon blood pump cycle from the heart. **b** Ventricular contraction and diastole during a heart pulse. **c** Diastolic and systolic stages incorporating P-, T-, and D-wave. Reproduced with permission from [28, 29]

peak pressure, respectively; and D-wave refers to the diastolic pulse waveform in the diastole stage [33]. These pulse wave peaks are important parameters to clinically validate cardiovascular conditions. For instance, quantitative indicators can be derived to assess the arterial stiffness corresponding to health status and age, including radial artery index, Air, defined as the amplitude ratio of P-wave and T-wave, and the time delay, ΔT_{DVP}, between the P-wave and T-wave peaks.

4.3 Heart Rate and Blood Pressure Monitoring Sensors

There are various types of sensing systems that are used in wearable heart pulse and blood pressure monitoring as summarized in Fig. 4. Therefore, a system classification can be applied based on the strain or displacement transducing mechanisms to record heart pulses and blood pressure. Wearable BPM devices adopt various physical sensing effects, aforementioned in Section 2 of this chapter, showing difference advantages/disadvantages that are applicable for variety of case scenarios.

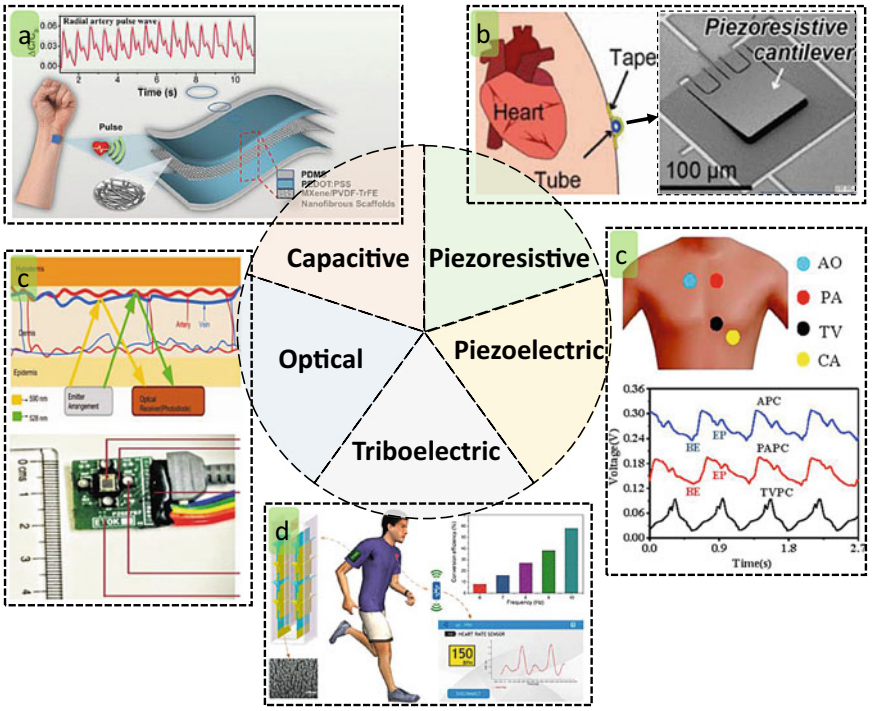

Fig. 4 Wearable heart pulse and blood pressure monitoring sensors with different sensing mechanisms: **a** Capacitive, **b** Piezoresistive, **c**, Piezoelectric, **d** Triboelectric/Nanogenerators, and **e** Optical

Capacitive effect-based BPM sensors are among the most commonly used owing to their low power operation and immunity to thermal noises from capacitive sensing elements. The capacitive readout and configuration can also be applied to a wide range of conductive and semiconductive materials making it widely adoptable in wearable BPM devices. As such, a MEMS capacitive pressure sensor element was used to detect arterial pulse waveform to predict atrial fibrillation [29]. The rated power consumption was reported as low as 5 μW at 3.3 V power supply and 100 kHz readout frequency, indicating the suitability for the long-term and continuous recording. Flexible nanocomposites were also preferable choices for capacitive BPM. A composite nanofibrous scaffold structure was reported with low-pressure detection limit and high stability across a wide pressure range [34]. Due to the soft nature of the composite, it exhibited good mechanical strength and resilience, high dielectric constant, and low hysteresis in radial artery pulse wave measurements.

Piezoresistive effect-based BPM sensors have been widely adopted for pulse wave monitoring due to the simple readout, wide range of material compatibility, and miniaturization. As such, a flexible multiplexed strain-gauge sensor fabricated from Pt-coated polymeric nanofibers was presented that can sense the heartbeat pattern [35]. Due to its highly directional selectivity and low detection range down to 5 Pa, the wearable sensor could accurately measure pressure variation in blood vessels while minimizing the cross-talk of shear strain by utilizing fiber-to-fiber contacts. This effect can also be utilized together with other biophysical signal recordings. A pressure-based miniaturized MEMS sensor with simultaneous measurement of pulse wave and respiration rate was successfully demonstrated [27]. The pressure sensor utilizes resistance change upon the bending of a micro cantilever structure to measure differential pressure down to 0.01 Pa. This extremely low-pressure threshold allows for the simultaneous recording of pulse wave and respiration rate when integrated in an eyeglass. However, it is still demanded for further developments to minimize their power consumption and thermal drift to make it more suitable for continuous BPM. Due to the transducer nature of the piezoresistivity, this type of BPM sensor does not require a power source which is preferable for continuous and wearable devices. Therefore, research efforts have been devoted to lower their frequency regime. A passive wearable BPM piezoelectric sensor was introduced with enhanced wearability, electric safety, and reliability [33]. The wearable device was able to measure radial pulsilogram and apex cardiogram with high signal-to-noise (SNR) ratio at the applicable frequency range of heart pulse patterns. The kind of BPM sensors can record the consecutive phases to identify the peaks including P-, T-, and D-waves of the cardiac pulse wave. Despite not requiring a power source, this type of BPM sensors is typically not capable in measuring at low frequencies (e.g., below 1 Hz), making it not universally usable for all BPM ranges.

Triboelectric nanogenerator-based BPM sensors is a new class of wearable devices that shows great potential for human health monitoring and specially BPM sensors. These devices can convert human motions during daily activities or exercise into electric power that are sufficient for powering sensing devices. This unique feature positions it as a promising candidate for wireless and self-power BPM devices. A triboelectric nanogenerator driven by wireless body sensor network real-time

human heart-rate monitoring [36]. The device could convert up to a maximum power of 2.28 mW from inertia energy when walking with a high conversion efficiency at 58%. However, the sensitivity and detection of this BPM type are still limited and require further research and development for new material and device integration.

Optical based BPM is the most widely adopted transducing mechanism in commercial products due to its ease of use. Researchers have been continuously optimizing system design and readout schemes to overcome these limitations. A 590 nm (yellow-orange) wavelength-based optical system was introduced for BPM devices [37]. At this chosen wavelength, there was improvement in the signal quality of PPG from varied skin tones, indicating the effective utilization of longer wavelength as optical emitters in the wrist-based wearable BPM. Due to significant influences by skin variations of the wearer such as colors and thickness, more efforts are still required to minimize the discrepancies in developing optical based BPM systems.

5 Respiratory Sensors

5.1 Importance of Respiratory Monitoring

Respiratory monitoring is a critical task in hospital settings, particularly for patients with respiratory issues, such as chronic obstructive pulmonary disease (COPD), asthma, and sleep apnea. Continuous monitoring of respiration will provide useful information about the respiratory rate, depth, pattern, and overall lung function of patients. Data collected from respiration assists healthcare professionals analyze and deal with respiratory disorders and assess treatment effectiveness, as well as identify potential problems.

Respiratory sensors are also used as an effective tool for early detection of respiratory issues. Their rapid and accurate monitoring of respiratory signals is essential for timely intervention and ensuring the safety of patients. Respiration sensors can detect abnormal breathing depth and rate and their deviations, patterns, or signs of respiratory distress. This early warning sign enables healthcare providers to act quickly and prevent severe problems, especially in anesthesia and in high-risk settings such as intensive care units [38].

In the optimization of sports performance, respiration monitoring will help athletes and coaches understand the impact of breathing activities on performance. Data is used to determine optimal breathing patterns during training and exercises and identify areas for improvement. Respiration sensors provide real-time signals and information about breathing rate and volume, allowing athletes to optimize their breathing duration for enhancing the endurance and maximizing their performance.

5.2 *Design of Respiration Sensors*

To accurately measure respiration signals, it is crucial to design wearable sensors capable of monitoring respiration with a high signal-to-noise ratio. These sensors operate based on the sensing mechanisms discussed in previous sections. They are capable of detecting various factors, including temperature, humidity, airflow velocity, as well as the movement of the chest and abdomen during breathing. The primary objectives in designing wearable respiration sensors are to ensure wearable functionality with high sensitivity and fast response. This necessitates careful selection of materials and structural designs to determine the sensors' sensitivity.

There are various types of systems that include wearable respiratory sensors available for monitoring respiration. These include the following.

Chest bands are a wearable device that is worn around the chest to monitor respiratory activity, Fig. 5. Respiratory sensors are integrated into the belts to detect the expansion and contraction of the chest during breathing. These sensors, often based on piezoelectric or strain gauge technologies, can measure the changes in the circumference of the chest as the user inhales and exhales. The detected movements are converted into electrical signals that can be analyzed to obtain information about respiration.

Sensor patches are wearable devices that are designed in the form of adhesive patches or sticker sensors that are applied directly to the body to monitor respiration, Fig. 5. These patches contain adhesive sensors and electronic components that can detect and measure various aspects of respiratory activity. These sensors typically work based on piezoelectric or capacitive effects, which are embedded within the patch and are in direct contact with the skin to capture the relevant signals. The special case of the sensor patches is a sensor that is attached to the philtrum and directly measure temperature or pressure, or flow induced by exhalation or inhalation.

In recent years, respiration sensors are integrated into a mask, Fig. 5. The sensors embedded in the mask can detect the airflow during breathing. They utilize various

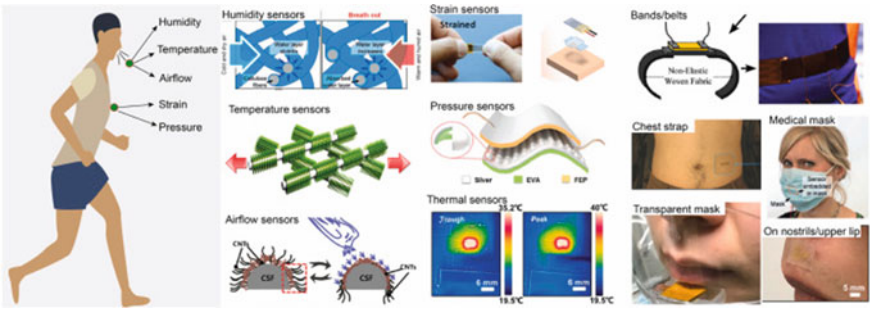

Fig. 5 Wearable respiratory sensors which are fixed in mask, incorporated into belts and patches to detect respiration activities (humidity, temperature, airflow, strain, and pressure). Reproduced with permission from [39]

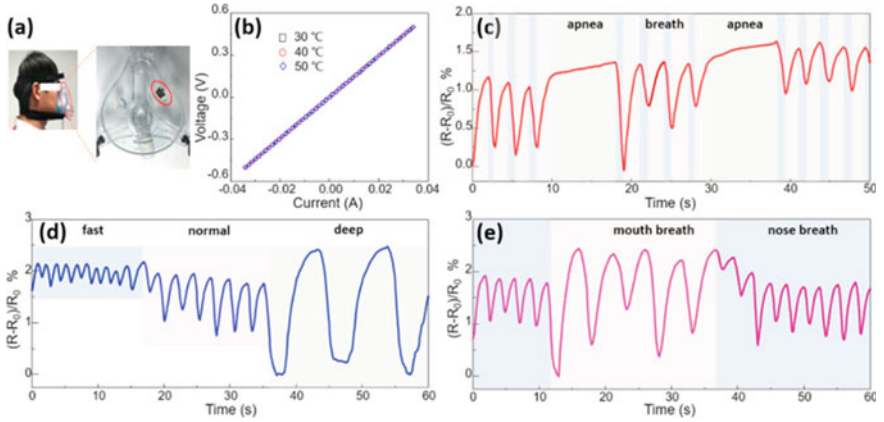

Fig. 6 A graphene respiration sensor that detects humidity changes. **a** The photograph of a graphene sensor attached in a medical breathing mask, **b** the current–voltage (I–V) characteristics of porous graphene network at different temperatures, **c** the resistance changes with breath and apnea, **d** the resistance changes to fast, normal, and deep breathing, **e** the resistance changes to breathing when fixed to mouth and nose. Reproduced with permission from [40]

sensing effect such as triboelectric, allowing the relevant respiratory signals to be captured with high sensitivity.

5.2.1 Humidity Sensors

The sensitivity of humidity-based respiration sensors depends on the selection of suitable materials. These sensors measure changes in humidity caused by breathing and require materials that are highly responsive to moisture variations. Designers consider materials with excellent hygroscopic properties, such as certain polymers or hydrogels, to enhance the sensitivity of the sensors to humidity changes associated with respiration. The typical structure of humidity sensors include a thin film or a porous three-dimensional structure [40]. Fig. 6 shows an example of a porous graphene-based humidity sensor which is incorporated into a medical breathing mask for monitoring of respiration [40] (also see Fig. 5 for medical masks used for humidity measurement). The sensor can detect normal, deep, fast and apnea [40].

5.2.2 Strain Sensors

The strain sensors are typically integrated into a belt or band (Fig. 5). Strain-based respiration sensors rely on detecting the deformation or stretching of the sensor caused by chest and abdominal movements during breathing [41]. Various structural designs are employed to improve the sensitivity of these sensors. This can include

incorporating specialized patterns or microstructures that respond to strain variations, allowing for more accurate and sensitive measurement of respiratory movements. Additionally, the use of advanced fabrication techniques, such as microelectromechanical systems (MEMS) or nanomaterials, can enhance the sensitivity of strain-based respiration sensors.

5.2.3 Pressure Sensors

Pressure sensors measure the flow-induced pressure on a sensing structure such as triboelectric fibers [42]. The development of pressure sensors for respiration monitoring has advanced toward self-powered sensing capability. Self-powered generation capability is a desirable feature in wearable respiration sensors. It allows the sensors to generate or harvest energy from the body movements or the surrounding environment, eliminating the need for external power sources or frequent battery replacements. This energy harvesting capability can be achieved through the integration of piezoelectric materials or triboelectric nanogenerators into the sensor design. Fig. 7 shows the recent design of respiration sensors based on the triboelectric effect induced between two fibers [42]. The sensors are typically integrated into a mask which converts the flow-induced pressure into electricity. These energy conversion mechanisms enable the sensors to convert mechanical motion or vibrations into electrical energy, ensuring long-term and sustainable operation.

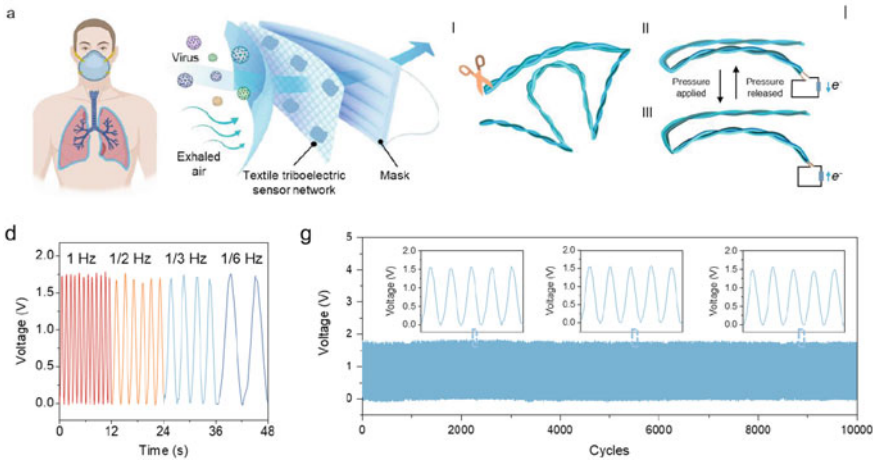

Fig. 7 Respiratory sensors embedded on mask based on triboelectric effect of fibers. **a** Wearable triboelectric sensors embedded on mask, **b** working principle of fiber-based triboelectric sensor, **c** response of sensor under different frequency, and **d** long-term stability of the sensor. Reproduced with permission from [42]

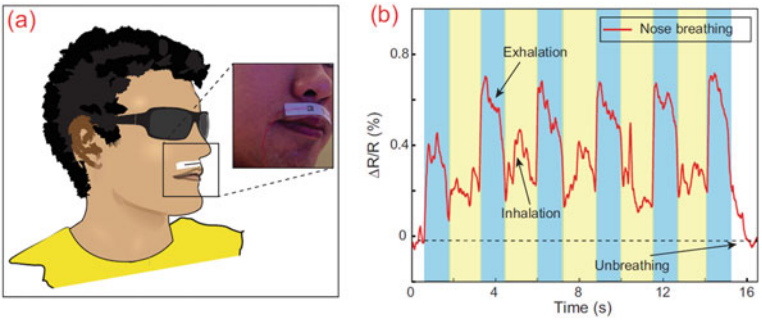

Fig. 8 Carbon nanotube fiber-based thermal sensor for respiration monitoring. **a** Sketch of a wearable thermal flow sensor affixed to human upper lip; **b** The resistance changes corresponding to nose breathing conditions. Reproduced with permission from [43]

5.2.4 Thermal and Flow Sensors

Exhalation leads to an increase in the temperature of the surrounding environments and increase in the airflow. To detect the temperature changes, temperature sensors can be utilized as respiration sensors. In order to achieve high-sensitivity measurement of respiration, hot-wire and hot-film thermal flow sensors can be employed. Hot-wire or hot-film flow sensors are supplied by a large electric current that causes a temperature rise due to the Joule heating effect. The breathing airflow cools the sensing elements (i.e., hot wire or hot film) down, and its resistance change (according to the piezoresistive effect) can be detected. Wearable thermal flow sensors are typically attached to human nostrils to enable the detection of these temperature changes. Fig. 8 shows a wearable thermal sensor using carbon nanotube yarn as a hot wire for measuring the direct airflow [43].

6 Conclusion

This chapter has provided an in-depth exploration of various physical sensing mechanisms and sensor technologies utilized in wearable devices for non-invasive health monitoring, including human motion monitoring, heart rate and blood pressure sensing, and respiratory monitoring. It also highlighted the significance of human motion monitoring, heart rate and blood pressure sensing, and respiratory monitoring in achieving continuous and accurate tracking of human physiological data. These advancements open up new possibilities for personalized health care, early disease detection, and improved overall health and life quality. As research and technology continue to evolve, wearable sensors are expected to play an increasingly vital role in transforming the way we monitor and manage our health. Further advancements in miniaturization, accuracy, and integration with other healthcare systems will enhance the capabilities of these sensors, enabling even more comprehensive

and precise monitoring. The potential for seamless integration with mobile applications and cloud-based IoT (Internet of Things) platforms will further empower individuals to take charge of their health, fostering a proactive approach to well-being. The journey toward transforming the way we monitor and manage our health is ongoing, and wearable sensors are at the forefront of this transformative wave.

References

1. Lide, D.R.: CRC Handbook of Chemistry and Physics. CRC press (2004)
2. Fiorillo, A.S., Critello, C.D., Pullano, S.A.: Theory, technology and applications of piezoresistive sensors: A review. Sens.S Actuators A: Phys. 281, 156–175 (2018). doi:https://doi.org/10.1016/j.sna.2018.07.006
3. Smith, C.S.: Piezoresistance effect in germanium and silicon. Phys. Rev. **94**(1), 42 (1954)
4. Bardeen, J., Shockley, W.: Deformation potentials and mobilities in non-polar crystals. Phys. Rev. **80**(1), 72 (1950)
5. Nguyen, C.T., et al.: Vertical piezo-optoelectronic coupling in 3C-SiC/Si heterostructure for self-powered and highly-sensitive mechanical sensing. ACS Appl. Mater. Interfaces (2023). doi:https://doi.org/10.1021/acsami.3c03045
6. Lazarus, N., Bedair, S.S., Lo, C.-C., Fedder, G.K.: CMOS-MEMS capacitive humidity sensor. J. Microelectromech. Syst. **19**(1), 183–191 (2009)
7. Riddle, B., Baker-Jarvis, J., Krupka, J.: Complex permittivity measurements of common plastics over variable temperatures. IEEE Trans. Microw. Theory Tech. **51**(3), 727–733 (2003)
8. Fastier-Wooller, J.W., et al.: Multimodal fibrous static and dynamic tactile sensor. ACS Appl. Mater. Interfaces (2022). doi:https://doi.org/10.1021/acsami.2c08195
9. Drobny, J.G.: Polymers for Electricity and Electronics: Materials, Properties, and Applications. John Wiley & Sons, (2012)
10. Md Foisal, A.R., et al.: Self-powered broadband (UV-NIR) photodetector based on 3C-SiC/Si heterojunction. IEEE Trans. Electron Devices 66(4), 1804–1809 (2019). doi:https://doi.org/10.1109/ted.2019.2899742
11. Wada, O., Nagai, K., Hiyama, Y., Nitta, S., Maruno, H., Mizuno, K.: Diabetes is a risk factor for restricted range of motion and poor clinical outcome after total knee arthroplasty. J. Arthroplasty **31**(9), 1933–1937 (2016)
12. Moeslund, T.B., Hilton, A., Krüger, V.: A survey of advances in vision-based human motion capture and analysis. Comput. Vis. Image Underst. **104**(2–3), 90–126 (2006)
13. Roriz, P., Ribeiro, A.B.L.: Fiber Optical Sensors in Biomechanics. In: Opto-Mechanical Fiber Optic Sensors, pp. 263–300. Elsevier (2018)
14. Kassanos, P., Rosa, B.G., Keshavarz, M., Yang, G.-Z.: From wearables to implantables-clinical drive and technical challenges." In: Wearable Sensors, pp. 29–84. Elsevier (2021)
15. Pizzolato, C., et al.: Bioinspired technologies to connect musculoskeletal mechanobiology to the person for training and rehabilitation. Front. Comput. Neurosci. **11**, 96 (2017)
16. Dao, D.V., Toriyama, T., Sugiyama, S.: Noise and frequency analyses of a miniaturized 3-DOF accelerometer utilizing silicon nanowire piezoresistors. SENSORS (2004)
17. Dao, D.V., Okada, S., Dau, V., Toriyama, T., Sugiyama, S.: Development of a 3-DOF silicon piezoresistive micro accelerometer. In: Micro-Nanomechatronics and Human Science and The Fourth Symposium Micro-Nanomechatronics for Information-Based Society (2004)
18. Alper, S.E., Azgin, K., Akin, T.: A high-performance silicon-on-insulator MEMS gyroscope operating at atmospheric pressure. Sens. Actuators A: Phys. 135(1), 34–42 (2007). doi:https://doi.org/10.1016/j.sna.2006.06.043
19. Wu, L., Tian, Z., Ren, D., You, Z.: A Miniature Resonant and Torsional Magnetometer Based on Lorentz Force. Micromachines (Basel) 9(2), (2018). doi:https://doi.org/10.3390/mi9120666

20. Muro-De-La-Herran, A., Garcia-Zapirain, B., Mendez-Zorrilla, A.: Gait analysis methods: An overview of wearable and non-wearable systems, highlighting clinical applications. Sensors 14(2), 3362–3394 (2014)
21. Aguirre, A., Sierra M, S.D., Munera, M., Cifuentes, C.A.: Online system for gait parameters estimation using a LRF sensor for assistive devices. IEEE Sensors J. 21(13), 14272–14280 (2021). doi:https://doi.org/10.1109/jsen.2020.3028279
22. Homayounfar, S.Z., Andrew, T.L., Wearable sensors for monitoring human motion: A review on mechanisms, materials, and challenges. SLAS Technol. 25(1), 9–24 (2020). doi:https://doi.org/10.1177/2472630319891128
23. Faisal, A.I., Majumder, S., Mondal, T., Cowan, D., Naseh, S., Deen, M.J.: Monitoring methods of human body joints: State-of-the-art and research challenges. Sensors (Basel) 19(11) (2019). doi:https://doi.org/10.3390/s19112629
24. Jeong, H., Rogers, J.A., Xu, S.: Continuous on-body sensing for the COVID-19 pandemic: Gaps and opportunities. Sci. Adv. 6(36) (2020)
25. Thomson, E.A., et al.: Heart rate measures from the Apple Watch, Fitbit Charge HR 2, and electrocardiogram across different exercise intensities. J. Sports Sci. **37**(12), 1411–1419 (2019)
26. Mizuki, Y., Nguyen, T.-V., Takahata, T., Shimoyama, I.: Highly sensitive pulse wave sensor with a piezoresistive cantilever inside an air chamber. In IEEE 32nd International Conference on Micro Electro Mechanical Systems (MEMS), 2019
27. Nguyen, T.-V., Ichiki, M.: MEMS-based sensor for simultaneous measurement of pulse wave and respiration rate. Sensors **19**(22), 4942 (2019)
28. Meng, K., et al.: Wearable pressure sensors for pulse wave monitoring. Adv. Mater. **34**(21), 2109357 (2022)
29. Kaisti, M., et al.: Clinical assessment of a non-invasive wearable MEMS pressure sensor array for monitoring of arterial pulse waveform, heart rate and detection of atrial fibrillation. NPJ Digit. Med. **2**(1), 39 (2019)
30. Lin, Q., et al.: Highly sensitive flexible iontronic pressure sensor for fingertip pulse monitoring. Adv. Healthcare Mater. 9(17), (2020). doi:https://doi.org/10.1002/adhm.202001023
31. Wang, X., Liu, Z., Zhang, T.: Flexible sensing electronics for wearable/attachable health monitoring. Small **13**(25), 1602790 (2017)
32. Lin, Q., et al.: Highly sensitive flexible iontronic pressure sensor for fingertip pulse monitoring. Adv. Healthcare Mater. **9**(17), 2001023 (2020)
33. Cai, F., et al.: Ultrasensitive, passive and wearable sensors for monitoring human muscle motion and physiological signals. Biosens. Bioelectron. **77**, 907–913 (2016)
34. Sharma, S., Chhetry, A., Sharifuzzaman, M., Yoon, H., Park, J.Y.: Wearable capacitive pressure sensor based on MXene composite nanofibrous scaffolds for reliable human physiological signal acquisition. ACS Appl. Mater. Interfaces **12**(19), 22212–22224 (2020)
35. Pang, C., et al.: A flexible and highly sensitive strain-gauge sensor using reversible interlocking of nanofibres. Nat. Mater. **11**(9), 795–801 (2012)
36. Lin, Z., et al.: Triboelectric nanogenerator enabled body sensor network for self-powered human heart-rate monitoring. ACS Nano 11(9), 8830–8837 (2017). doi:https://doi.org/10.1021/acsnano.7b02975
37. Mohapatra, P., Preejith, S., Sivaprakasam, M.: A novel sensor for wrist based optical heart rate monitor. In: IEEE International Instrumentation and Measurement Technology Conference (I2MTC) (2017)
38. Mirjalali, S., Peng, S., Fang, Z., Wang, C.H., Wu, S.: Wearable sensors for remote health monitoring: Potential applications for early diagnosis of covid-19. Adv. Mater. Technol. 7(1), 2100545 (2022). doi:https://doi.org/10.1002/admt.202100545
39. Dinh, T., Nguyen, T., Phan, H.-P., Nguyen, N.-T., Dao, D.V., Bell, J.: Stretchable respiration sensors: Advanced designs and multifunctional platforms for wearable physiological monitoring. Biosens. Bioelectron. 112460 (2020)
40. Pang, Y., et al.: Wearable humidity sensor based on porous graphene network for respiration monitoring. Biosens. Bioelectron. **116**, 123–129 (2018)

41. Ho, M.D., et al.: Percolating network of ultrathin gold nanowires and silver nanowires toward "invisible" wearable sensors for detecting emotional expression and apexcardiogram. Adv. Func. Mater. **27**(25), 1700845 (2017)
42. Fang, Y., et al.: A deep-learning-assisted on-mask sensor network for adaptive respiratory monitoring. Adv. Mater. **34**(24), 2200252 (2022)
43. Dinh, T., et al.: Environment-friendly carbon nanotube based flexible electronics for noninvasive and wearable healthcare. J. Mater. Chem. C **4**(42), 10061–10068 (2016)